Autophagy

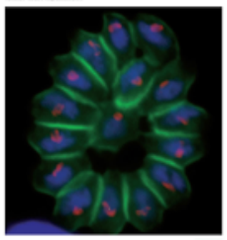

Autophagy

ISSN: 1554-8627 (Print) 1554-8635 (Online) Journal homepage: informahealthcare.com/journals/kaup20

Trehalose delays the progression of amyotrophic lateral sclerosis by enhancing autophagy in motoneurons

Karen Castillo, Melissa Nassif, Vicente Valenzuela, Fabiola Rojas, Soledad Matus, Gabriela Mercado, Felipe A. Court, Brigitte van Zundert & Claudio Hetz

To cite this article: Karen Castillo, Melissa Nassif, Vicente Valenzuela, Fabiola Rojas, Soledad Matus, Gabriela Mercado, Felipe A. Court, Brigitte van Zundert & Claudio Hetz (2013) Trehalose delays the progression of amyotrophic lateral sclerosis by enhancing autophagy in motoneurons, Autophagy, 9:9, 1308-1320, DOI: 10.4161/auto.25188

To link to this article: https://doi.org/10.4161/auto.25188

Autophagy 9:9, 1308–1320; September 2013; © 2013 Landes Bioscience

Trehalose delays the progression of amyotrophic lateral sclerosis by enhancing autophagy in motoneurons

Karen Castillo,[1,2] Melissa Nassif,[1,2] Vicente Valenzuela,[1,2] Fabiola Rojas,[3] Soledad Matus,[4] Gabriela Mercado,[1,2] Felipe A. Court,[4,5] Brigitte van Zundert[3] and Claudio Hetz[1,2,4,6]

[1]Biomedical Neuroscience Institute; Faculty of Medicine; University of Chile; Santiago, Chile; [2]Center for Molecular Studies of the Cell; Program of Cellular and Molecular Biology; Institute of Biomedical Sciences; University of Chile; Santiago, Chile; [3]Center for Biomedical Research; Faculty of Biological Sciences and Faculty of Medicine; Universidad Andrés Bello; Santiago, Chile; [4]Neurounion Biomedical Foundation; Santiago, Chile; [5]Millennium Nucleus for Regenerative Biology; Faculty of Biology; Pontificia Universidad Catolica de Chile; Santiago, Chile; [6]Department of Immunology and Infectious Diseases; Harvard School of Public Health; Boston, MA USA

Keywords: amyotrophic lateral sclerosis, copper-zinc superoxide dismutase 1, trehalose, protein aggregation, autophagy

Abbreviations: ALS, amyotrophic lateral sclerosis; SOD1, copper-zinc superoxide dismutase 1; MAP1LC3B or LC3, microtubule-associated protein 1 light chain 3 beta; FOXO1, forkhead box protein O1; MTOR, mechanistic target of rapamycin

Amyotrophic lateral sclerosis (ALS) is a fatal motoneuron disease with no current effective treatment. Accumulation of abnormal protein inclusions containing SOD1, TARDBP, FUS, among other proteins, is a pathological hallmark of ALS. Autophagy is the major degradation pathway involved in the clearance of damaged organelles and protein aggregates. Although autophagy has been shown to efficiently degrade ALS-linked mutant protein in cell culture models, several studies suggest that autophagy impairment may also contribute to disease pathogenesis. In this report, we tested the potential use of trehalose, a disaccharide that induces MTOR-independent autophagy, in the development of experimental ALS. Administration of trehalose to mutant SOD1 transgenic mice significantly prolonged life span and attenuated the progression of disease signs. These effects were associated with decreased accumulation of SOD1 aggregates and enhanced motoneuron survival. The protective effects of trehalose were associated with increased autophagy levels in motoneurons. Cell culture experiments demonstrated that trehalose led to mutant SOD1 degradation by autophagy in NSC34 motoneuron cells and also protected primary motoneurons against the toxicity of conditioned media from mutant SOD1 transgenic astrocytes. At the mechanistic level, trehalose treatment led to a significant upregulation in the expression of key autophagy-related genes at the mRNA level including *Lc3*, *Becn1*, *Sqstm1* and *Atg5*. Consistent with these changes, trehalose administration enhanced the nuclear translocation of FOXO1, an important transcription factor involved in the activation of autophagy in neurons. This study suggests a potential use of trehalose and enhancers of MTOR-independent autophagy for the treatment of ALS.

Introduction

Amyotrophic lateral sclerosis (ALS) is the most common motoneuron disease in adults, characterized by the selective loss of motoneurons in motor cortex, brain stem and spinal cord. ALS is presently incurable and patients undergo progressive paralysis with an average survival upon diagnosis from one to five years.[1,2] The majority of ALS cases lacks a defined hereditary genetic component and are considered sporadic (sALS), while approximately 10% of cases are familial (fALS). Mutations in superoxide dismutase 1 (*SOD1*), TAR DNA binding protein (*TARDBP/TDP-43*), fused-in-sarcoma/translated-in-liposarcoma (*FUS*), among other proteins have been associated with fALS.[3] Although the mechanism underlying ALS pathogenesis is unclear, aggregation of ALS-linked mutant proteins is thought to contribute to motoneuron dysfunction through alteration of diverse cellular processes (see examples in ref. 4). Moreover, recent studies suggest that protein inclusions observed in sALS cases contain misfolded forms of wild-type TARDBP, FUS, or SOD1.[5-7] Although the factors controlling the misfolding and aggregation of these proteins in ALS are not well defined, strategies to decrease the load of unfolded proteins in ALS represent an interesting target for disease intervention.

The ubiquitin–proteasome and autophagy–lysosomal pathways are the main routes for protein degradation. Lysosomes can degrade large substrates such as protein complexes, aggregates and organelles through macroautophagy (here referred to as autophagy). Several studies have demonstrated that most

*Correspondence to: Claudio Hetz; Email: chetz@med.uchile.cl and chetz@hsph.harvard.edu
Submitted: 12/05/12; Revised: 05/22/13; Accepted: 05/27/13
http://dx.doi.org/10.4161/auto.25188

aggregation-prone mutant proteins linked to neurodegeneration are efficient substrates for autophagy-mediated degradation.[8] Autophagy involves the formation of double-membrane structures known as autophagosomes where cargos are engulfed. These vesicles eventually fuse with lysosomes where their content is degraded by acidic lysosomal hydrolases.[9] We and others have described the upregulation of autophagy markers in spinal cord tissue derived from sALS and fALS patients,[10-12] in addition to mouse models of the disease.[10-15] Although many independent studies indicate an efficient degradation of mutant SOD1 or TARDBP by autophagy in cell culture,[15-19] no direct validation is available in favor for a therapeutic benefit of targeting the pathway in ALS in vivo. Genetic or pharmacological manipulations that provide protection against ALS had been only correlated with autophagy induction in mouse models.[11,20-22] It is still a matter of debate where or not autophagy activation has beneficial effects in ALS or if its impairment may represent a pathological mechanism underlying neurodegeneration.[23] Besides, growing evidence suggests that autophagy activity may be impaired in several neurodegenerative diseases including ALS. For example, recent genetic screening in ALS identified mutations in proteins involved in the regulation of autophagy, including SQSTM1 and UBQLN2.[24,25] ALS-linked mutations in charged multivesicular body protein-2B (*CHMP2B*) or the lipid phosphatase also trigger alterations in the autophagy pathway.[25,26] In agreement with these observations, genetic inactivation of autophagy in the central nervous system results in spontaneous neurodegeneration, involving the accumulation of protein aggregates and extensive neuronal loss.[27,28] These studies suggest that defects in the protein homeostasis network are part of the etiology of ALS.

The MTOR pathway is the best-characterized regulator of autophagy initiation upon nutrient starvation. The enhancement of autophagy by inhibition of MTOR with rapamycin protects against experimental Parkinson and Huntington disease, associated with the degradation of mutant SNCA/α-synuclein or HTT/Huntingtin, respectively.[29] Rapamycin administration also reduces cognitive defects of an experimental model of Alzheimer disease, decreasing fibrillary tangles and amyloid plaques associated with autophagy induction.[30] The possible impact of rapamycin to ALS progression was recently tested in two independent studies. Unexpectedly, although treatment of mutant *SOD1* transgenic mice with rapamycin led to increased levels of autophagy markers in the spinal cord, this strategy accelerated the progression of the disease, associated with exacerbated motoneuron apoptosis with no evident effects in mutant SOD1 levels.[31] These results may be explained by the pleiotropic effects of MTOR signaling in many different processes including regulation of mRNA translation, transcription, cell growth and metabolism, and inflammation among other functions.[32] The negative effects of rapamycin administration in ALS may even reflect an actual impairment of autophagy fluxes in mutant *SOD1* transgenic mice, where further stimulation of the pathway triggers the abnormal accumulation of cargoes/vesicles.[33] In contrast, another study has not detected any effect of rapamycin administration to an ALS mouse model.[34] In the search for novel autophagy regulators, pharmacological screenings by Rubinsztein's group have revealed the existence of distinct MTOR-independent mechanisms to initiate autophagy involving fluctuations in inositol or calcium levels (reviewed in ref. 35). Trehalose is a natural disaccharide with chemical chaperone activity that specifically engages MTOR-independent autophagy by an unknown mechanism. Trehalose treatment induces the degradation of diverse aggregate-prompt proteins through autophagy in cell culture models.[36-40] Moreover, trehalose treatment has important neuroprotective effects in animal models of Parkinson disease, Alzheimer disease, oculopharyngeal muscular dystrophy and Huntington disease.[41-44] Remarkably, trehalose is bioactive in these diseases even through oral administration, reducing protein aggregation and improving neuronal survival and motor performance. Only a few recent studies have associated the neuroprotective effects of trehalose with autophagy induction in vivo in models of Tau-mediated pathology and Alzheimer disease.[43-45] Based on this evidence, here we explored the possible use of trehalose for the treatment of ALS and its relation to autophagy induction. Our results demonstrated a therapeutic impact of trehalose in extending life span of mutant *Sod1* transgenic mice, increasing motoneuron survival associated with decreased mutant SOD1 aggregation possibly due to autophagy induction. Cell culture experiments using NSC34 cells and primary motoneurons demonstrated protective effects of trehalose treatment against ALS features. At the molecular level, we showed that trehalose treatment upregulates the expression of a variety of essential autophagy-regulatory genes, in addition to enhance the nuclear translocation of forkhead box O1 (FOXO1), an important transcription factor involved in the regulation of autophagy in neurons.[46-48] Our results suggest that targeting MTOR-independent autophagy may have therapeutic benefits in ALS.

Results

Trehalose treatment increases life span and delays disease onset of mutant SOD1 transgenic mice. To determine the possible effects of trehalose administration to the development of ALS, we used the SOD1^{G86R} transgenic mice, which expressed an enzymatically inactive protein under the control of the endogenous *Sod1* promoter. We performed intraperitoneal injections of 2 g/Kg trehalose three times per week and complemented this treatment with free consumption in the drinking water (3% w/v). As control, an identical regimen was performed using 2 g/Kg glucose or sucrose. Additional control animals were injected with an equivalent volume of PBS (untreated). All treatments started at the asymptomatic phase of the disease (around 35 d of age), until the terminal stage of the disease. Remarkably, we observed a significant extension of life span of SOD1^{G86R} transgenic mice treated with trehalose when compared with the two control groups (**Fig. 1A**). Interestingly, analysis of the survival curves by gender revealed that the protective effects of trehalose were stronger in male than female mice. An increase in average survival of approximately 32 d in males compared with approximately 15 d in female mice was observed in animals treated with trehalose compared with PBS injected controls (**Fig. 1B–D**). Glucose (**Fig. 1A–C**) or sucrose (not shown) administration did

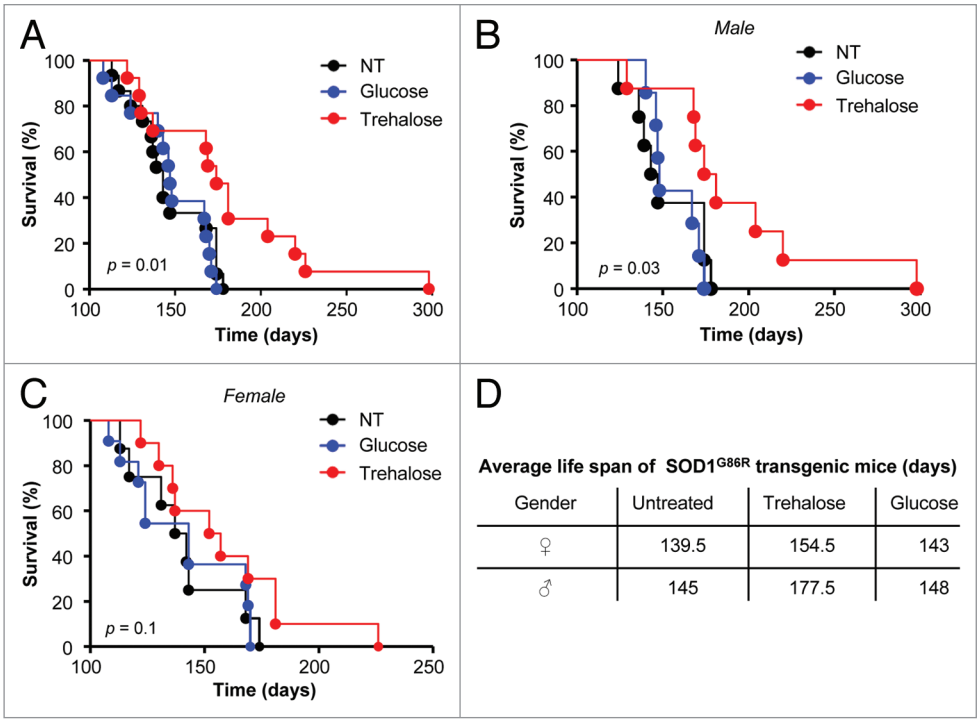

Average life span of SOD1^{G86R} transgenic mice (days)

Gender	Untreated	Trehalose	Glucose
♀	139.5	154.5	143
♂	145	177.5	148

Figure 1. Trehalose treatment prolongs the life span of mutant SOD1 transgenic mice. (**A**) SOD1^{G86R} transgenic mice were intraperitoneally injected with 2 g/Kg of trehalose (n = 17), 2 g/Kg of glucose (n = 15) or an equivalent volume of PBS (untreated, n = 15) starting at 35 d of age. The compounds were also permanently provided in a concentration of 3% in the drinking water (free consumption). Mouse survival was monitored over time. Animals presented in A were divided into groups of male (**B**) and female (**C**) mice. Total group numbers for male mice: trehalose (n = 9), glucose (n = 7) and untreated (n = 8). Females: trehalose (n = 8), glucose (n = 8) and untreated (n = 7). (**D**) Average life span of animals treated with trehalose, glucose or PBS injected is presented. Survival curves were estimated by Kaplan-Meier statistic analysis. In (**A–C**), the p value was calculated with log-rank test (Mantel-Cox) to compare trehalose with PBS treated animals.

not have any significant effect on the life span of SOD1^{G86R} transgenic mice when compared with PBS-injected mice.

To monitor disease onset and progression in mutant SOD1 transgenic mice, we measured body weight loss, rotarod performance and the appearance of visual disease signs starting at 90 d of age (see criteria in Materials and Methods and **Fig. S1A and S1B**). Using all these parameters, we observed that trehalose treatment led only to a slight tendency to delay disease onset in male and female SOD1^{G86R} mice that was not statistically significant (**Fig. 2A–C**). Remarkably, analysis of the progression of disease severity indicated that trehalose administration considerably attenuated the progression of ALS-related signs of SOD1^{G86R} transgenic animals (**Fig. 2D**; **Fig. S1C**). While control animals died on average 4 d after disease onset (**Fig. S1D**), reaching a score over 20 (late stage symptomatic disease), trehalose-treated animals displayed mild to moderate disease signs for a longer time, reaching higher values close to the end point of the disease (**Fig. 2D**; **Fig. S1C**). Taken together, these results indicate that trehalose treatment significantly extends the life span of mutant SOD1 transgenic mice involving a slower progression of disease signs compared with control animals.

As additional control experiment, we determined the possible effects of the chronic treatment of mice with trehalose/glucose in blood glycemia and glucose tolerance. We fasted animals for 2 h (two consecutive days) and measured glucose levels in blood after intraperitoneal injection 2 g/kg glucose in mutant SOD1 animals treated with trehalose or glucose. No alterations in glycemia were observed (**Fig. S2A and S2B**), excluding possible effects on glucose homeostasis in our drug-testing regimen.

Trehalose treatment decreases the levels of SOD1 aggregation in vivo. We then measured the accumulation of mutant SOD1 aggregates in spinal cord samples of SOD1^{G86R} transgenic mice. Trehalose treatment led to a reduction in the overall levels of SOD1 oligomers as measured by western blot analysis, whereas glucose administration did not have any effect (**Fig. 3A**). Quantification of these experiments revealed a consistent and statistically significant reduction of SOD1 aggregation after treatment with trehalose, both in males and females at similar levels (**Fig. 3B**; **Fig. S3A**). Similar results were obtained when frontal cortex from the same animals was analyzed (**Fig. S3B**). Mutant SOD1 monomers were also decreased after trehalose treatment as determined by quantification of the protein in spinal cord samples of trehalose-treated animals compare with controls (**Fig. S3C**). As a control we also measured the mRNA levels of *Sod1*, where no changes were observed after trehalose treatment (**Fig. S3D**).

We also performed a general histopathological characterization of the spinal cord of mutant SOD1 transgenic mice to visualize glial activation and motoneuron survival. We determined the levels of astrocyte activation after GFAP staining and confocal microscopy. As shown in **Figure 3C**, trehalose treatment had a significant effect in reducing glial activation of mutant SOD1 mice. In addition, we measured motoneuron survival in the ventral horn by toluidine blue staining of mutant SOD1 mice treated with trehalose or PBS (littermate controls) at the time of disease onset. An overall protection was observed in animals treated with trehalose that was confirmed after quantification of motoneurons, identified by their distribution in the ventral horn, their size and morphology (**Fig. 3D**). These results were confirmed after staining with the neuronal marker RBFOX3/NeuN (not shown). In summary, these results suggest that the effects of trehalose treatment on the progression of experimental ALS are associated with decreased levels of mutant SOD1 aggregation, reduced astrocyte activation and improved motoneuron survival.

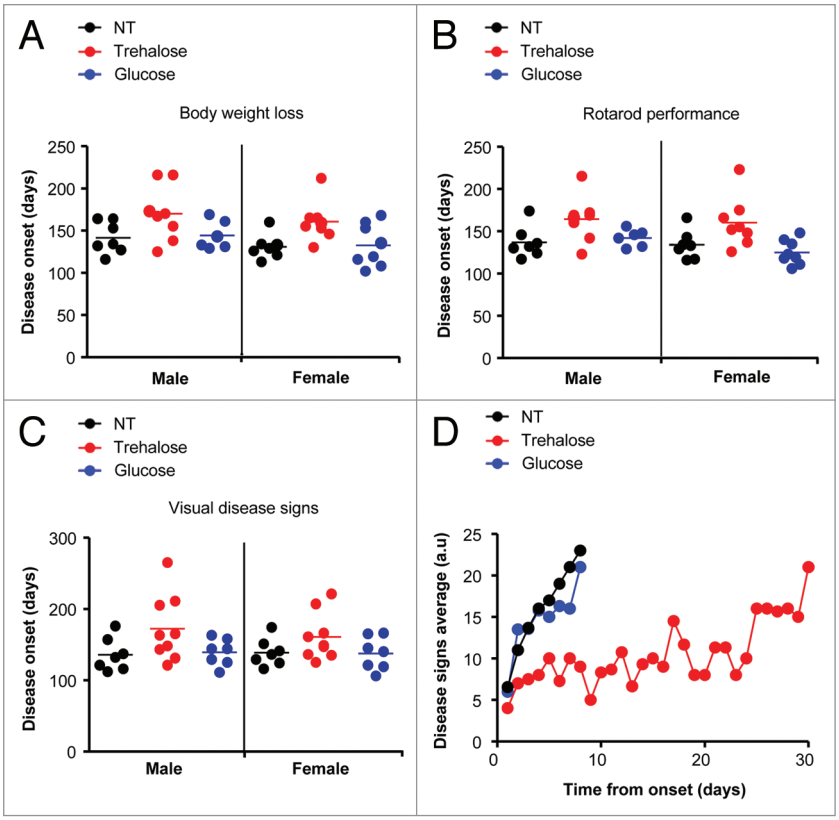

Figure 2. Trehalose treatment ameliorates the progression of disease signs in mutant SOD1 transgenic mice. (**A**) Disease onset was monitored in SOD1^{G86R} animals described in **Figure 1** after treatment with trehalose, glucose or PBS. Disease onset was calculated as the day when animals lost 5% of their total body weight. (**B**) In parallel, rotarod performance was monitored as described in Materials and Methods to determine disease onset. (**C**) The appearance of several disease signs was assessed to obtain a disease score and evaluate the progression of the severity of the disease. A minimum value of 3 was used to define disease onset. Scored parameters included the appearance of spinal curvature, signs of paralysis, slight hind limbs tremor, ruffling fur and falling of hind limbs (see **Fig. S1A and S1B**). In (**A–C**) no statistically significant differences were determined between the experimental groups using Student's t-test. (**D**) Average disease progression of mutant SOD1 transgenic animals treated with trehalose, glucose and untreated, as indicated, by visual observation of disease signs. Number of animals used per group: trehalose (n = 7, male; n = 5 female), glucose (n = 6, male; n = 5 female) or an equivalent volume of PBS (n = 4, male; n = 3 female). Statistical analysis of disease duration is presented in **Figure S1C**.

Trehalose induces autophagy in mutant SOD1 transgenic mice. To assess the possible impact of trehalose in autophagy levels, we measured microtubule-associated protein 1 light chain 3 β (MAP1LC3B, hereafter LC3) expression in spinal cord extracts from late stage symptomatic ALS mice. One of the key steps in the regulation of autophagy is the conjugation of cleaved LC3 to phosphatidylethanolamine to form LC3-II. Cleaved and lipidated LC3 binds to the expanded phagophore and remains associated with autophagosomes even after fusion with lysosomes. Monitoring conversion into LC3-II, LC3 distribution as puncta (autophagosomes), or its flux through the autophagy pathway are among the most widely accepted gold standards to measure autophagy activity in the field. Trehalose treatment induced a significant increase in total levels of LC3 and its cleaved and lipidated form LC3-II (**Fig. 4A**; **Fig. S4A**). In addition, we visualized the number of neurons containing LC3-positive puncta (more than 3 dots/neuron) in the spinal cord of SOD1 transgenic mice using immunofluorescence (**Fig. 4C**). In agreement, NeuN-positive neurons in mutant SOD1 mice presented increased LC3-positive dots in the presence of trehalose (**Fig. 4C**). In this analysis, we also corroborated the increase in total LC3 levels (diffuse staining) upon administration of trehalose (**Fig. 4C**). Moreover, the autophagy substrate SQSTM1 was also upregulated in mutant SOD1 mice, which were reduced in trehalose-treated animals (**Fig. 4B**). Finally, since trehalose has been proposed to induce MTOR-independent autophagy,[35] we monitored the levels of phospho-MTOR and its substrate RPS6KB2 (also known as p70S6 kinase 2) in trehalose-treated mice. We did not observe any change in the phosphorylation status of these two proteins in spinal cord extracts from mutant SOD1 transgenic mice in any treatment (**Fig. 4D** and not shown). As a positive control, NSC34 cells were exposed to nutrient starvation, which triggered clear MTOR-dephosphorylation (**Fig. 4D**). Taken together, these results suggest that the protective effects of trehalose administration in vivo are associated with the induction of autophagy in motoneurons.

Trehalose enhances the transcription of autophagy-regulatory genes and the activation of FOXO1. Although trehalose is one of the few known compounds to induce MTOR-independent autophagy with effective activity in animal models,[35] its mechanism of action is completely unknown. Because trehalose treatment increased total LC3 levels (**Fig. 4A and C**), we decided to measure its mRNA levels by quantitative PCR. Trehalose administration, and not glucose, led to a strong induction of *Lc3* mRNA levels in both female and male mutant SOD1 transgenic mice (**Fig. 5A**). Because of these unexpected results, we then examined the mRNA levels for other key autophagy regulatory genes including *Sqstm1*, *Becn1*, *Atg5* and *Atg7* in late stage symptomatic animals (**Fig. 5A** and not shown). Since *Sqstm1* mRNA levels were enhanced whereas SQSTM1 proteins levels reduced (**Fig. 4B**), trehalose treatment may trigger a strong degradation of SQSTM1 protein suggesting enhanced autophagy flux in vivo. There was a significant increase in the expression of all these autophagy genes in the spinal cord of ALS mice upon trehalose administration when compared with glucose or PBS control group (**Fig. 5A**). In addition, significant induction of the mRNA level of some of these genes was observed in the spinal cord and brain cortex of presymptomatic mutant SOD1 mice treated with trehalose (**Fig. S4B**).

Based on our gene expression results, we investigated the levels of two stress responsive transcription factors that have been

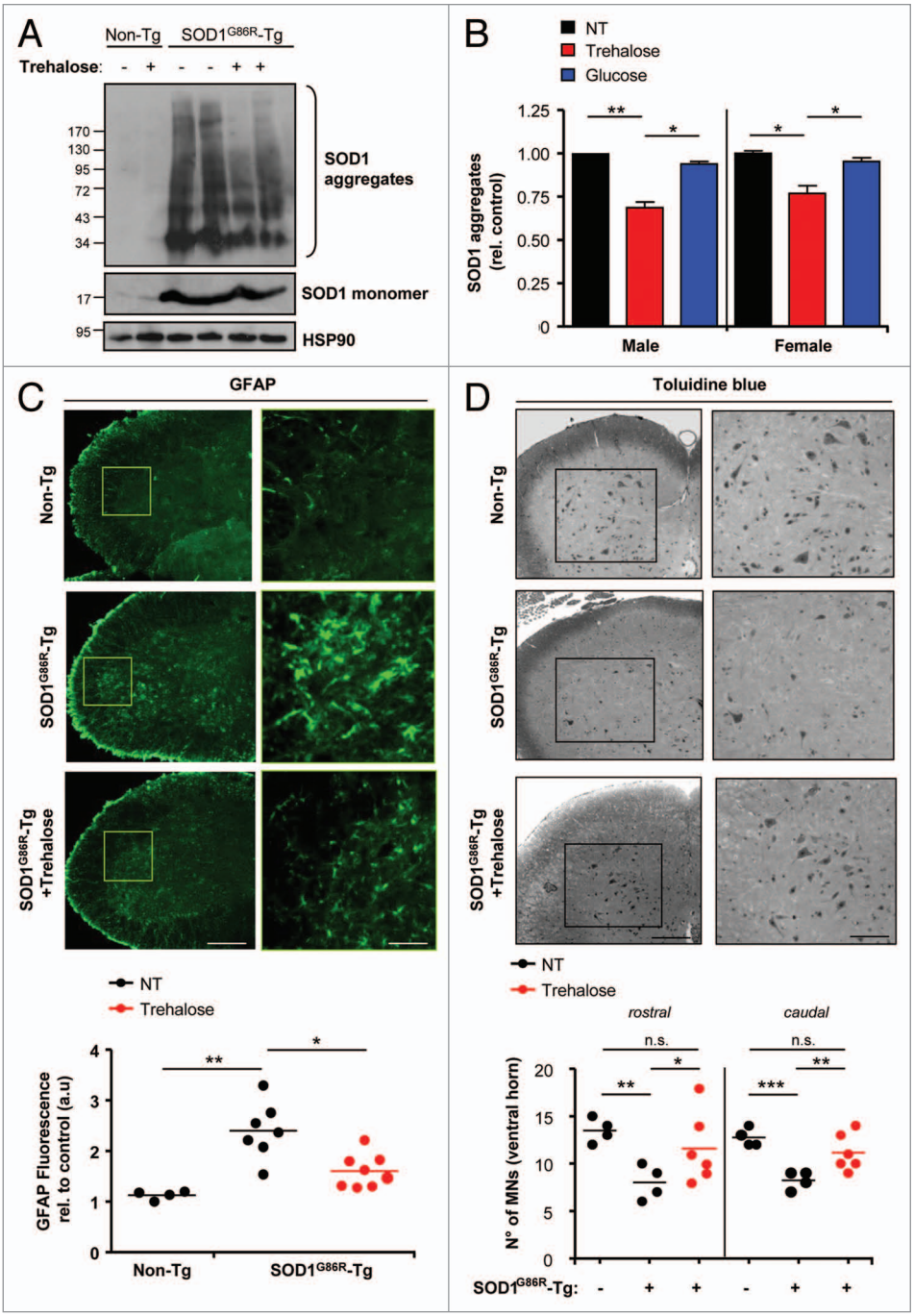

Figure 3. Trehalose administration decreases mutant SOD1 aggregation, reduces astrogliosis and improves neuronal survival. (**A**) SOD1 aggregation was determined in spinal cord protein extracts derived from SOD1^{G86R} transgenic mice treated with trehalose, glucose or PBS. Each track represents one independent animal. Tissue was collected at the symptomatic phase of the disease. HSP90 was monitored as a loading control. Image was assembled from cropped lanes of the same western blot analysis. (**B**) Quantification mutant SOD1 aggregation levels in spinal cord extracts normalized with the loading control from (**A**) and **Figure S3A**. Number of animals analyzed per treatment in male and female mice respectively: Trehalose (n = 8 and 7), glucose (n = 7 and 6) and PBS (n = 8 and 8). (**C**) Immunofluorescence analysis of GFAP staining in spinal cord tissue derived from animals described in **Figure 1** at the symptomatic stage of the disease. Upper panel: A representative image is shown of the analysis of four independent animals. A zoom is presented at the left of the selected area on a rectangle. (Scale bar: 250 μm and 60 μm). Bottom panel: quantification of GFAP signal is shown (see methods). (**D**) Motoneuron survival was determined in the ventral horn of the spinal cord after toluidine blue staining. Motoneurons were identified by their distribution, morphology and size. Tissue was collected in animals at 120 d of age. Littermate control mice were used for the analysis. In all panels with statistical analysis mean and standard deviation (**B**) or mean is presented with a line (**C and D**). p values were calculated with Student's t-test, *p < 0.01; **p < 0.005; ***p < 0.0005. n.s.: non-significant.

recently shown to control the expression of a similar group of autophagy genes, Forkhead box O1 (FOXO1)[46-49] and activating transcription factor 4 (ATF4).[50-52] ATF4 levels were not induced in spinal cord of mutant SOD1 mice after trehalose treatment as assessed by western blot analysis (not shown), consistent with the fact that AFT4 deficiency does not affect LC3 levels in mutant SOD1 mice.[53] In contrast, we detected an enhancement of the nuclear translocation of FOXO1 (a sign of activation) in spinal cord samples of late stage symptomatic mutant SOD1 mice treated with trehalose when compared with glucose or PBS treated animals (**Fig. 5B**). Glucose treatment had a slight effect as previously described in paradigms of metabolic diseases.[54] Overall, our results revealed a possible mechanism of action of trehalose where it can trigger the upregulation of a subset of autophagy-regulatory genes and the activation of FOXO1, a key regulator of autophagy in the nervous system.

Trehalose enhances autophagy-mediated degradation of mutant SOD1 in NSC34 motoneuron cells. Our results suggest a direct correlation between (1) the protective effects of trehalose administration in ALS mouse models, (2) the upregulation of autophagy and (3) a decrease in the levels of mutant SOD1 aggregation. Because of the impossibility of measuring autophagy flux/activity in vivo in the nervous system due to the lack of reliable methods,[55] we validated the impact

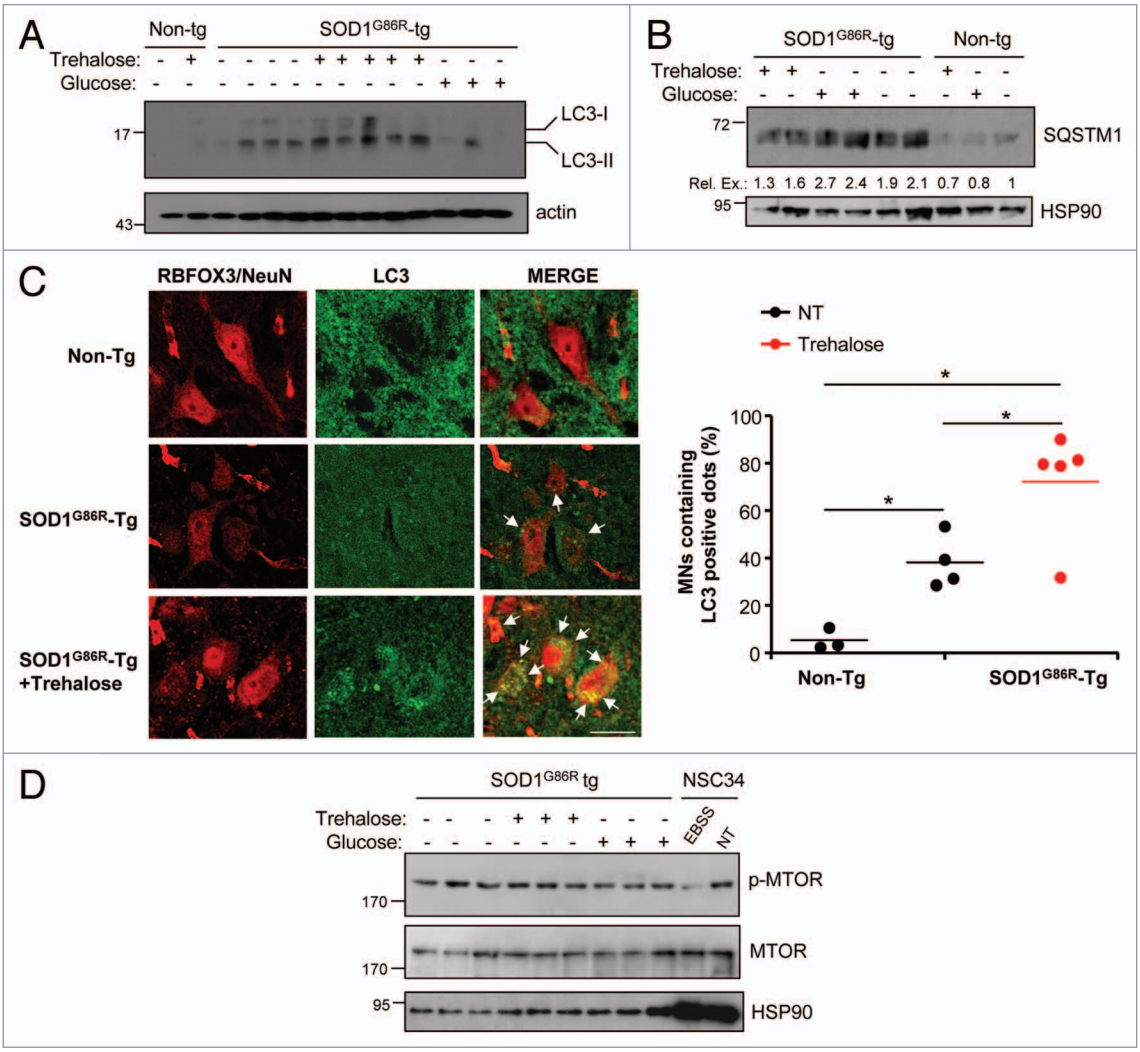

Figure 4. Treatment of mutant SOD1 transgenic mice with trehalose induces autophagy in spinal cord motoneurons. (**A**) LC3 expression was determined in spinal cord samples derived from SOD1^{G86R} transgenic or nontransgenic mice (Non-Tg) treated with trehalose, glucose, or PBS. Tissue was collected at the symptomatic phase of the disease. HSP90 levels were monitored as loading control. Each well represents an independent animal. (**B**) In parallel, SQSTM1 levels were monitored by western blot. The relative expression (Rel. Ex.) level in each well was quantified and normalized to HSP90 and presented as a fold induction in comparison with the expression observed in nontransgenic untreated animals. (**C**) LC3 distribution was assessed by indirect immunofluorescence (green) in motoneurons of animals treated as described in **Figure 1**. Motoneurons were identified after staining with RBFOX3/NeuN (red), in combination with the identification of their morphology, size and distribution (left panel). Right panel: The percentage of RBFOX3/NeuN-positive neurons containing LC3 positive dots (> 3 puncta per cell) was quantified. Mean is presented with a line. p values were calculated with Student's t-test, *p < 0.01 (Scale bar: 20 μm). (**D**) Phosphorylation of MTOR was determined by western blot in samples presented in A. Total MTOR and HSP90 were analyzed as control. As positive control, NSC34 motoneuron cells were treated with EBSS to induce nutrient starvation and analyzed in the same gel.

of trehalose on autophagy and mutant SOD1 degradation on a cellular model. ALS pathogenesis involves both cell-autonomous effects (i.e., direct perturbation of motoneuron function) and cell-nonautonomous components (i.e., production of neurotoxic species by astrocytes).[2,56] To monitor the impact of trehalose on SOD1 degradation, we transiently expressed human SOD1^{G85R} fused to EGFP in the motoneuron cell line NSC34. We then assessed the effects of trehalose treatment on mutant SOD1 aggregation using western blot analysis. We performed treatments with 100 mM trehalose 2 h before or 24 h after transfection. A dramatic decrease in mutant SOD1 aggregation was observed in both settings of trehalose treatment (**Fig. 6A**). Moreover, similar to our observations in vivo, monomeric mutant SOD1 species were also decreased after trehalose administration (**Fig. 6A**). Trehalose treatment also increased the targeting of mutant SOD1 to LC3-positive vesicles as measured by immunofluorescence and confocal microscopy analysis (**Fig. 6B**). In all of these experiments trehalose treatment induced autophagy as measured by monitoring LC3-II levels (**Fig. 6A**) or LC3-positive autophagosomes (**Fig. 6B**).

To determine if the decrease in mutant SOD1 levels by trehalose treatment is due to enhanced autophagy, we treated cells with the general autophagy inhibitor 3-methyladenine (3-MA, which blocks the PtdIns3K initiation complex).[57] Treatment of cells with

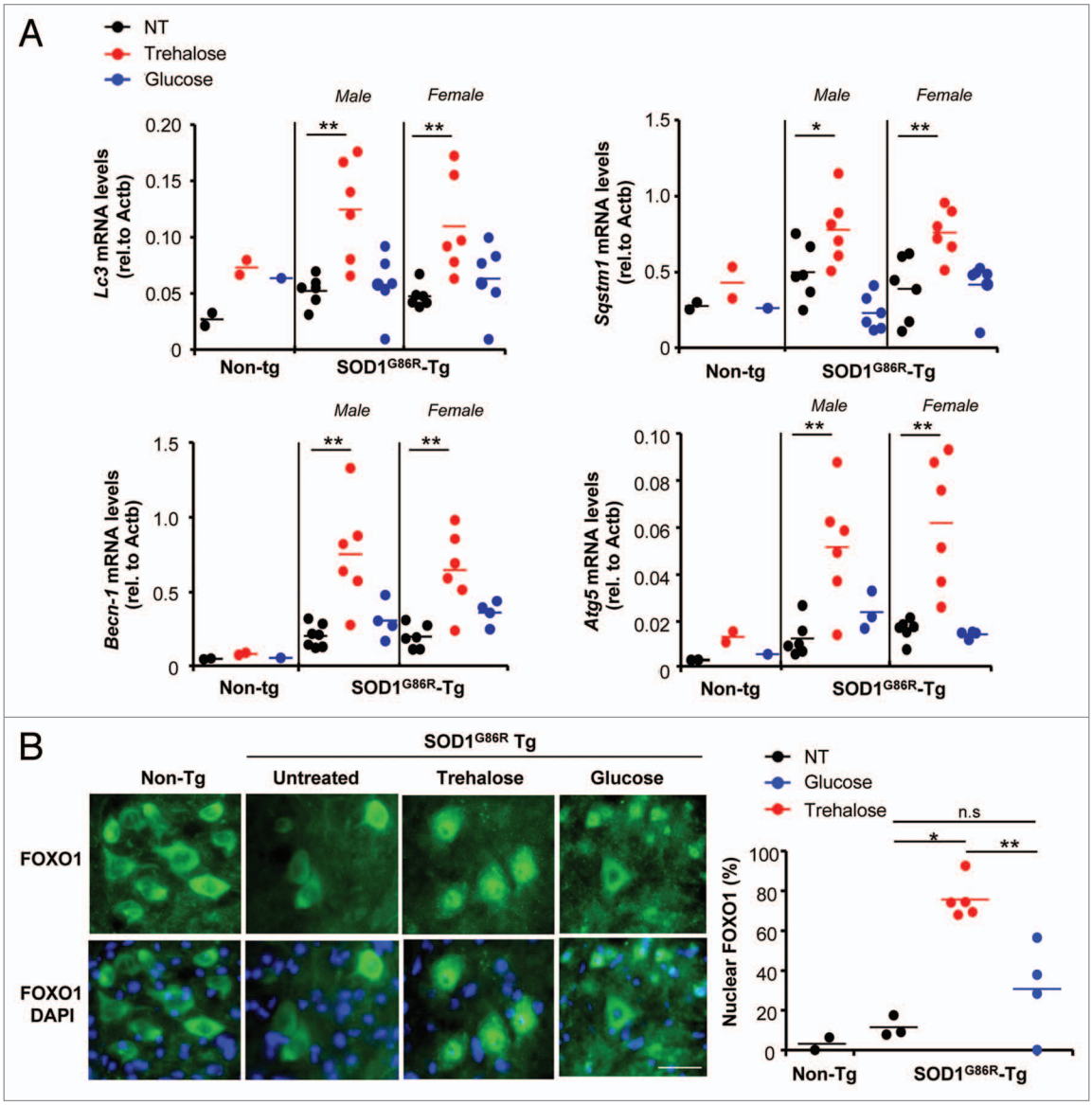

Figure 5. Trehalose modulates the expression of a cluster of autophagy-regulatory genes and the activation of FOXO1. (**A**) Spinal cord tissue from mutant SOD1 transgenic mice treated with trehalose, glucose or PBS was collected at the symptomatic phase of the disease and relative mRNA levels of indicated genes was analyzed by real-time PCR using total cDNA. As control, non-transgenic animals were also analyzed. Male and female mice were analyzed. Values were normalized with β-actin (*Actb*) levels. Mean is presented with a line. (**B**) Right panel: The subcellular distribution of FOXO1 was assessed by immunofluorescence analysis (green) of spinal cord tissue of animals described in (**B**) (Scale bar: 40 μm). Right panel: The number of cells presenting nuclear localization of FOXO1 was quantified per area in the ventral horn of the spinal cord. Littermate controls were used for the analysis. Mean is presented with a line. In (**A–C**), p values were calculated with Student's t-test, *p < 0.01; **p < 0.005. n.s.: nonsignificant.

3-MA reverted the effects of trehalose on the expression levels of mutant SOD1 aggregates and monomers (**Fig. 6C**). Similarly, treatment of cells with a cocktail of lysosomal inhibitors (200 nM bafilomycin A_1, 10 μg/ml pepstatin, 10 μg/ml E64d) restored mutant SOD1 aggregation after trehalose treatment (**Fig. 6C**). Interestingly, trehalose treatment also partially reduced the accumulation of mutant SOD1 in the presence of autophagy inhibitors, suggesting the occurrence of autophagy-independent effects on the degradation of SOD1. Finally, we confirmed the induction of autophagy flux by trehalose in NSC34 cells using the mCherry–GFP-LC3 reporter (**Fig. 6D**). Together, these results indicate that trehalose treatment induces the degradation of mutant SOD1 by autophagy.

Trehalose protects against the cell-nonautonomous effects of glia over primary motoneurons. In addition to the intrinsic effects of ALS-mutant genes on motoneurons, many important studies revealed that astrocytes expressing mutant SOD1 produce toxic species that alters motoneuron function and viability (examples in).[58-60] We prepared primary astrocyte cultures from newborn mutant SOD1 mice and collected conditioned media (ACM) after 3 weeks of culture. Then, we exposed wild-type embryonic primary rat motoneurons to ACM for 4 d and

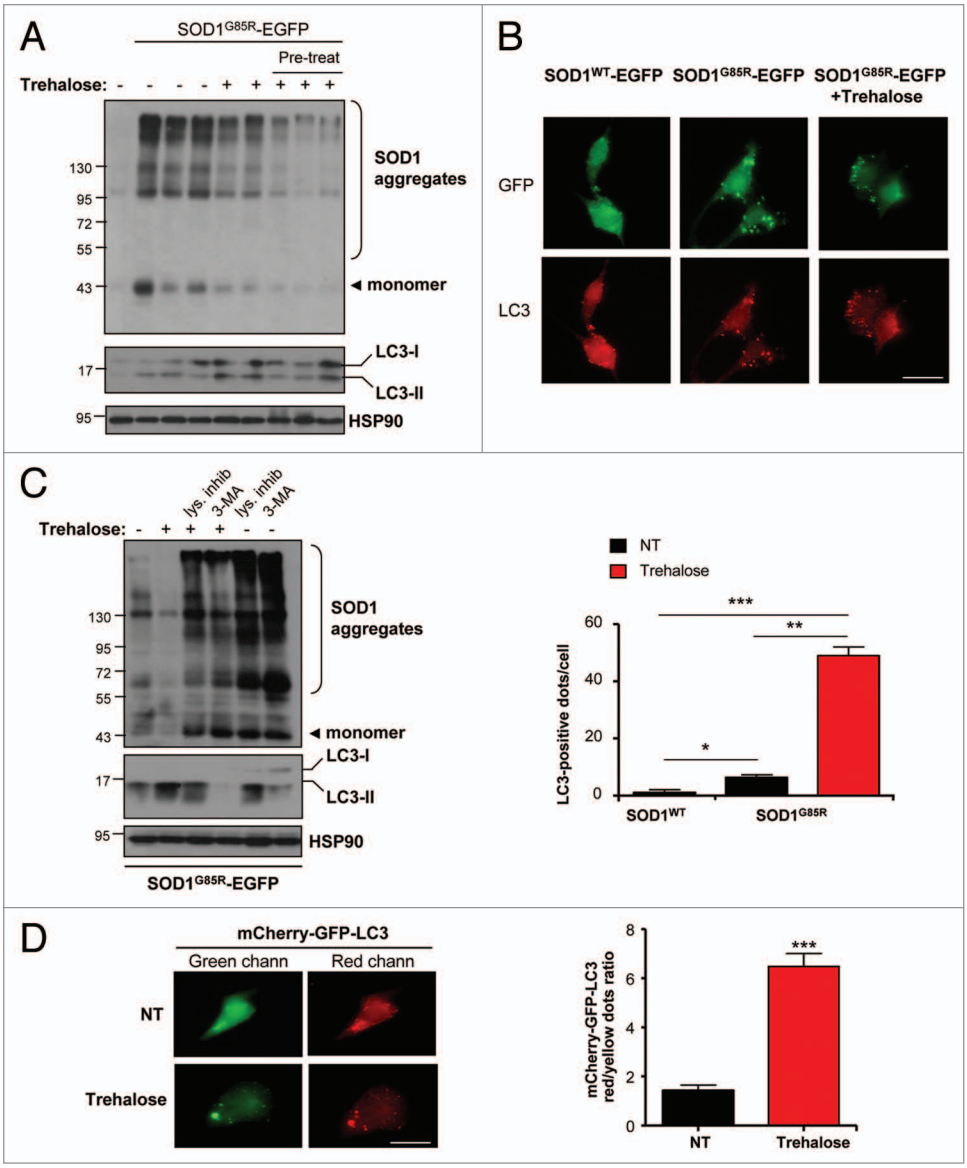

Figure 6. Trehalose triggers autophagy-mediated degradation of mutant SOD1 in NSC34 motoneuron cells. (**A**) NSC34 cells were transiently transfected with an expression vector for human SOD1^{G85R} fused to EGFP. Cells were cotreated for 48 h or preincubated 24 h before transfection with 100 mM trehalose. SOD1 aggregates were visualized by western blot analysis. Each well represents an independent experiment. SOD1^{G85R} monomers are also indicated. Bottom panels: The levels of LC3 and HSP90 (loading control) were monitored in the same samples. (**B**) Immunofluorescence analysis of endogenous LC3 (red) and SOD1^{G85R}-EGFP (green) using spinning disk microscopy. As control, NSC34 cells were transiently transfected with SOD1^{WT}-EGFP (upper panel). Lower panel: The number of cells containing LC3-positive dots was quantified. Mean and standard deviation is presented. Scale bar: 20 μm. (**C**) NSC34 cells were transiently transfected with an expression vector for SOD1^{G85R}-EGFP and treated with or without 100 mM trehalose. In addition, cells were exposed to a cocktail of lysosomal inhibitors (200 nM bafilomycin A_1, 10 μg/ml pepstatin, 10 μg/ml E64d) or 10 mM 3-methyladenine (3-MA). Then, the levels of mutant SOD1 aggregation and the monomeric form were determined by western blot. As control for the treatments, LC3 expression was determined. (**D**) To monitor autophagy fluxes in the absence of inhibitors, NSC34 cells were transiently transfected with an expression vector for mCherry-GFP-LC3 and treated with or without 100 mM trehalose. Then, the presence of GFP-mCherry- (i.e., autophagosomes) and mCherry-positive (i.e., autolysosomes) dots were visualized using spinning disk microscopy. Right panel: quantification of the ratio between red vs. yellow dots to assess an autophagy flux index. Mean and standard error is presented. p values was calculated with Student's t-test, *p < 0.01; **p < 0.005; ***p < 0.0005.

measured motoneuron viability. As previously reported using this ALS in vitro model,[58,61] treatment of motoneurons with ACM from mutant SOD1 transgenic astrocytes reduced the viability of motoneurons as visualized by MAP2 and NEFH (known as SMI-32) costaining (**Fig. 7A and B**). Remarkably, trehalose treatment significantly protected motoneurons against ACM toxic effects (**Fig. 7B**). These effects correlated with the induction of LC3-positive dots in the mix culture treated with trehalose (**Fig. 7C**). These results are also consistent with the known impact of autophagy and trehalose treatment in decreasing stress levels and inhibiting cell death.[36,62]

Discussion

Here we provide evidence in favor of a protective role of autophagy in ALS progression in vivo. ALS is presently incurable and the only approved drug for disease treatment is riluzole which has marginal effects on symptoms and patient survival.[63] A hallmark of most neurodegenerative conditions is the presence of abnormally folded proteins that accumulate and aggregate in specific areas of the brain leading to neuronal dysfunction and death. Based on this transversal feature of neurodegenerative diseases, targeting autophagy to reduce proteotoxicity represents an interesting target for the development of more efficient treatments.[64] Autophagy is critical for the maintenance of protein homeostasis in the nervous system. This is evidenced by the fact that the specific ablation of the autophagy-related genes *Atg5* or *Atg7* in neurons results in spontaneous neurodegeneration.[27,28] In agreement with these findings, several reports suggest that defects in the autophagy pathway may contribute to neurodegeneration in diverse CNS diseases.[8]

Although many studies suggest that autophagy operates as an efficient mechanism to eliminate

potentially neurotoxic species of mutant SOD1 and TARDBP, in vivo studies have only correlated the activation of autophagy with neuroprotection in ALS mouse models.[11,20-22] For example, we described that targeting the ER stress transcription factor XBP1 induces autophagy and delays ALS, and possibly Huntington disease, due to degradation of mutant SOD1[11] or HTT[46] respectively. Because of its beneficial effects in models of neurodegeneration, rapamycin was explored as a possible strategy to induce autophagy-dependent protection in ALS. Despite positive expectations, rapamycin had no effects or even strong detrimental consequences on mutant SOD1 mouse survival and disease progression.[31,34] Since the MTOR pathway has broad effects in many cellular pathways, the negative effects reported by Zhang et al. may be due to interference with processes controlled by MTOR that are not directly related to autophagy. Therefore, rapamycin may not be recommended as a safe drug to be tested in ALS patients. Interestingly, recently rapamycin treatment was shown to protect against TARDBP pathogenesis in vivo in a model of frontotemporal lobar dementia and ALS, improving cognitive defects associated with the induction of autophagy markers.[65] Lithium, a molecule used to treat psychiatric disorders, alleviated degeneration in one study against mutant SOD1 pathogenesis in mice, correlating with the upregulation of autophagy markers.[20] Lithium induces MTOR-independent autophagy possibly through modification of inositol levels.[35] In contrast to this study, other reports have not found any positive effects of lithium administration in ALS.[66-69] Trehalose has been shown only recently to induce neuroprotection involving enhanced autophagy in mouse models of Taupathies and Alzheimer disease.[43-45] Other studies described therapeutic effects of trehalose in vivo in brain diseases, but the impact of autophagy in the process was not evaluated. Trehalose is normally found, for example, in yeast, insects and flies during development, and in other organisms where it may have a stabilizing activity on protein structures and membranes against a variety of stresses possibly due to its "chemical chaperone" properties. Many chemical chaperones have been identified, such as 4-PBA and TUDCA, which provide protection against protein folding stress in neurodegenerative conditions possibly due to an attenuation of protein aggregation and decreased ER stress.[70] In contrast, levels of ER stress markers were not attenuated in our ALS model by treating animals with trehalose (**Fig. S5**), suggesting that the beneficial effects of trehalose may not be related to its chemical chaperone activity in our experimental model. However, we cannot exclude that the chemical chaperone activity of trehalose, in addition to the induction of autophagy, contributes to its neuroprotective effects in vivo. Trehalose treatment not only decreased aggregated forms of mutant SOD1 but also the levels of its monomer, which is consistent with the concept that autophagy also degrades soluble forms of misfolded-mutant proteins as we and others have suggested.[46,64] This effect may be also important in ALS because monomeric forms of mutant SOD1 are highly diffusible and neurotoxic.[71]

Here, we demonstrate a significant protection in ALS by the pharmacological stimulation of autophagy using an orally active drug. Surprisingly, trehalose treatment increased the life span of mutant SOD1 mice without affecting disease onset. The progression of the severity of disease signs, however, was attenuated in animals treated with trehalose. The impact of trehalose on mutant SOD1 transgenic mice survival was significant in both male and female mice, having a more potent protection in male animals. This observation is interesting because ALS has a higher incidence in men. However, the molecular mechanism underlying this differential susceptibility in human patients to develop ALS is unknown. The effects of trehalose in autophagy levels were always more evident in transgenic mice when compared with littermate control wild-type animals, suggesting that the induction of autophagy by trehalose may involve a crosstalk between signaling events triggered by this compound and the cellular responses induced by the accumulation of mutant SOD1. We observed a remarkable effect of trehalose in autophagy levels in spinal cord motoneurons after combining the delivery of the drug through oral administration and intraperitoneal injection. This result contrasts with recent observations in a Tau transgenic mice, where few effects of trehalose were reported in the spinal cord.[44] In that study, trehalose was only delivered in the drinking water, which may explain the poor efficacy of the drug. In addition, here we showed that trehalose had a greater effect in mutant SOD1 male mice, which is relevant because ALS has a higher incidence in male patients. Similarly, we have also reported that a genetic manipulation that alters autophagy and ER protein homeostasis in SOD1 mutant mice is gender-dependent.[11]

The mechanism of action explaining the activation of MTOR-independent autophagy by trehalose is unknown. Our results identify a possible pathway and suggest that trehalose administration induces the upregulation of a network of key autophagy genes at the transcriptional level which correlates with the activation of FOXO1, a key transcription factor involved in the regulation of autophagy in neurons. We are currently investigating if FOXO1 is directly involved in the expression of autophagy genes by trehalose administration. Importantly, there are no reports indicating detrimental effects of trehalose in humans, and the FDA approved this drug for future testing because of its regular used as a preserving agent in the food industry. Overall, our results suggest that stimulation of MTOR-independent autophagy represents an interesting target for future development of therapeutic strategies to treat ALS.

Materials and Methods

Animal experimental procedures. To model ALS we used transgenic mice expressing mouse SOD1^{G86R} on a C57BL76 background. This mutant is equivalent to the human *SOD1*^{G85R} mutation and encodes an enzyme with low SOD1 activity that is controlled by the endogenous *Sod1* promoter. Trehalose was obtained from Tokio Chemicals Industry CO (T0331) and Sigma (T9449). Trehalose, sucrose, or glucose was administrated by intraperitoneal injections (2 g/Kg) three times per week in animals around 35 d after birth. In addition, to increase the efficacy of the drug treatments were complemented by delivery of 3% w/v trehalose or glucose in the drinking water (ad libitum).

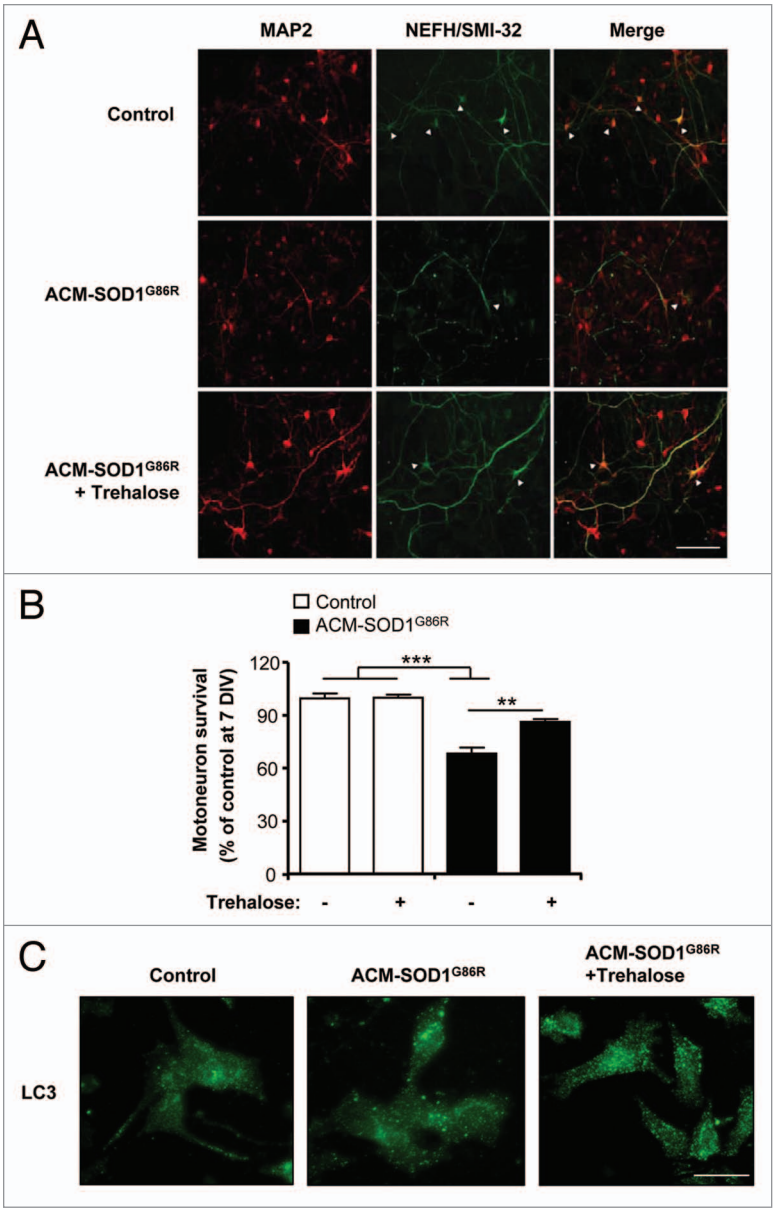

Figure 7. Trehalose reduces the death of primary motoneurons against conditioned media from mutant SOD1 transgenic astrocytes. (**A**) Cell culture media was conditioned for 7 d (from 2 to 3 weeks) by astrocytes derived from transgenic mice overexpressing SOD1^{G86R} (ACM-SOD1^{G86R}). Primary rat spinal cord cultures (3 DIV) were exposed to ACM-SOD1^{G86R} for 4 d alone or with trehalose (175 mM) and fixed at 7 DIV to assay cell survival with immunocytochemistry. Cultures were fixed at 7 DIV and double-labeled with anti-MAP2 antibody (red) to visualize interneurons and motoneurons and with the anti-NEFH/SMI-32 antibody (green) to identify motoneurons (arrow). Scale bar: 200 μm. (**B**) The percentage of motoneuron survival was quantified in experiments presented in A. Values represent means and standard error from three independent experiments performed in duplicate. ***$p < 0.001$ relative to control media in the absence or presence of trehalose (white bars) and analyzed by one-tailed t-test followed by a Welch post hoc test. **$p < 0.007$ relative to ACM-SOD1^{G86R} with trehalose (black bar) and analyzed by Student's t-test. (**C**) LC3 distribution was analyzed by immunofluorescence in experiments presented in (**A**).

Disease onset was determined using (1) the rotarod assay, (2) by measurement body weight loss (5% body weight loss) and (3) through visual observation of disease signs using methods previously described.[11,72] Disease progression was estimated by scoring disease parameters including falling of the hind limbs, curvature of spine, slight tremor of hind limbs, ruffling fur, hunched posture and paralysis (see details scores in **Fig. S1**). For the control of glycemia in animals treated with sugars, blood samples were collected from the tail vein of animals that were fasted for 2 h and then injected with 2 g/Kg glucose through intraperitoneal injection. Blood glucose levels and glycemia were assesses with the glucometer system Accu-Chek (Roche Diagnostics). General guideline for experimental in vivo use of ALS mouse models were followed as suggested in.[73] All animal experiments were performed according to procedures approved by the Institutional Review Board's Animal Care of the Faculty of Medicine of the University of Chile.

Tissue extraction and analysis. For histopathological analysis, spinal cord tissue was collected and processed for immunohistochemistry using standard procedures as we previously described.[74] Spinal cord tissue was processed for immunohistochemistry using standard procedures as described.[75] In brief, mice were sacrificed and spinal cord or whole brain was fixed with 4% paraformaldehyde in 0.1 M saline phosphate buffer (PBS). A small section (1 cm) of lumbar spinal cord tissue was collected and homogenized in Triton X-100 containing a protease inhibitor cocktail (Roche) by sonication, for biochemical analysis. The fixed spinal tissue was subjected to a sucrose gradient (5%, 10% and 30% sucrose in PBS), cryoprotected with Optimal Cutting Temperature compound (Tissue Tek), and fast frozen using liquid nitrogen. Sections of 30 μm were immunostained using antibodies anti-RBFOX3/NeuN (Millipore, MAB377) 1:100; anti-FOXO1 (Abcam, 12161), 1:100; and anti-GFAP (Dako, N1506) 1:1000. Quantification of motoneurons was performed using ultrathin sections and toluidine blue staining, followed by visualization on a light microscope as described before,[55,76] and images were captured using a QImaging QICAM Fast 1394 camera. Confocal microscopy was used to acquire immunofluorescence images following analysis with the Image J Software (http://rsbweb.nih.gov/ij). For western blot analysis antibodies and dilutions used were as follows: LC3B (Cell Signaling, 2775S), Phospho-p70S6-K/RPS6KB2 (Cell Signaling, 9205), p70S6-K/RPS6KB2 (Cell Signaling, 9202), Phospho-MTOR (Cell Signaling, 2971), MTOR (Cell Signaling, 2983), 1:2000; SQSTM1 (Abcam, ab56416), 1:10000; FOXO1 (Abcam, ab12161), 1:1000; HSP90 (Cell Signaling, 7947),1:4000; SOD1 1:3000 (Calbiochem, 574597); PDIA1/PDI (Enzo, spa891) 1:2000; ERp72 (Enzo, spa720) 1:1000; CNX/calnexin (Enzo, spa860) 1:1000; HSPA5/BiP (Enzo, spa826) 1:1000.

Methods for real-time PCR analysis were described before.[74] Primer sequences are as follows: *Lc3* forward: GCC TCG CAG

GAG ACA TTC GGG, *Lc3* reverse: TGT GGG TGG TGA GCC GTC CA; *Sqstm1* forward: CGA TGA CTG GAC ACA TTT GTCT, *Sqstm1* reverse: GTC CTT CCT GTG AGG GGT CT; *Becn1* forward: GAG CCA TTT ATT GAA ACT CGC CA, *Becn1* reverse: CCT CCC CGA TCA GAG TGAA; *Atg5* forward: AGA GTC AGC TAT TTG ACG TTGG, *Atg5* reverse: TGG ACA GTG TAG AAG GTC CTT TT; *Atg7* forward: GTT CGC CCC CTT TAA TAG TGC, *Atg7* reverse: TGA ACT CCA ACG TCA AGC GG; *Atg12* forward: CCC CGG AAC GAG GAA CTC CCG, *Atg12* reverse: GGA TGG TCC GGG TTC GCT CCA; *Foxo1* forward: GTG GCT TTG TGG CTC TGT CCT GG, *Foxo1* reverse: AGA GCC AAA GAG AAC AGA GGT GGGG; *Actb* forward: CTC AGG AGG AGC AAT GAT CTT GAT, *Actb* reverse: TAC CAC CAT GTA CCC AGG CA; *Sod1* forward: GCC CGC TAA GTG CTG AGTC, *Sod1* reverse: CCA GAA GGA TAA CGG ATG CCA.

Measurements of autophagy. Different assays and control experiments were performed to monitor autophagy following the recommendations and precautions described in the cited reference 55. Autophagy was monitored by analyzing LC3-positive dots through histological analysis or by the measurement of LC3-II levels using western blot as we previously described.[11] For cell culture experiments, the motoneuron cell line NSC34 was employed according to previously reported cell culture conditions.[77] LC3 flux was measured by treating cells with cocktail of lysosomal inhibitors including 200 nM bafilomycin A_1, 10 μg/mL pepstatin and 10 μg/mL E64d. Alternatively, LC3 flux was measured in cell culture by the transient transfection of an expression vector for the tandem monomeric mCherry-GFP-tagged LC3 following analysis that was previously described.[78]

Primary neuronal cultures, astrocytes conditioned media and cell death. Astrocytes conditioned media (ACM) was prepared as described before.[61] In brief, cultures of astrocytes were prepared from P1-2 wild-type mice and from transgenic mice expressing $SOD1^{G86R}$. Cultures were maintained in DMEM (Hyclone SH30081.02) containing 10% FBS (Hyclone SH30071.03; lot ATC31648) and 1% penicillin-streptomycin (Invitrogen, 15070-063) at 37°C 5% CO_2. Cultures reached confluence after approximately 14 d and contained > 95% $GFAP^+$ astrocytes. Residual microglia cells were removed by shaking in an orbital shaker (200 r.p.m. in the incubator) for 6 h. Next, media was replaced by spinal culture media (see below). After 7 d (21 DIV), ACM was collected, centrifuged (500 g for 10 min) and stored at −80°C. Before use, the ACM was supplemented with 4.5 mg/ml D-glucose (final concentration) and penicillin/streptomycin and filtered. We also added a chick hind limbs muscle extract.[79] ACM was diluted 10-fold (10%); at this concentration ACM-$hSOD1^{G86R}$ strongly reduced motoneuron survival, whereas control ACM was not toxic.

Pregnant Sprague-Dawley rats were used to prepare primary spinal cultures from E14 pups as described before.[79] For treatments, primary spinal cultures were fixed at 7 DIV with 4% paraformaldehyde, and immunostained with an antibody against MAP2 (1:400; Santa Cruz Biotechnology) to visualize all neurons (interneurons as well as motoneurons); immunostaining with the NEFH/SMI-32 antibody (Covance, AMI-32R, 1:600) revealed the presence of unphosphorylated neurofilament-H, expressed specifically in motoneurons in spinal cord cultures.[58] Previously we found that our wild-type primary spinal cultures typically contain 6–10% motoneurons until 12 DIV.[79] Fluorescent neurons were visualized with epifluorescent illumination on an Olympus IX81 microscope (Olympus America Inc.), or on a Nikon C1 confocal microscope (Nikon Instruments Inc.) on which stacks of 0.50 μm optical sections were acquired through entire neurons. MAP2- (Santa Cruz Biotechnology, 20172, 1:300) and NEFH-positive neurons were counted offline within 20 randomly chosen fields, and the percentage of NEFH-positive motoneurons within the total number of MAP2-positive cells was calculated. Each condition was replicated in at least 3 independent cultures, and in duplicate.

Disclosure of Potential Conflicts of Interest

The authors declare no conflict of interest in this study.

Acknowledgments

We thank Omar Ramirez for helping with image analysis and Monica Perez for tissue preparation and toluidine blue staining. We thank Silke Escobar for managing the animal colony. This work was funded by the Muscular Dystrophy Association and ALS Therapy Alliance; Millennium Institute no. P09-015-F, FONDECYT no. 1100176, ACT1109; and FONDEF D11I1007 (C.H.). We also thank the Michael J. Fox Foundation for Parkinson Research, Alzheimer Disease Association (C.H.). In addition we received support from to FONDECYT no. 1110987 and Millennium Nucleus no. P07-011-F (F.C.); FONDECYT Postdoctoral fellowship no. 3120146 (G.M.) and no. 3100112 (K.C.); FONDECYT 11121524 (S.M.); and ALS Therapy Alliance, Ring Initiative ACT1114 and FONDECYT no. 1101012 (B.vZ.). V.V. and M.C. received a CONICYT PhD fellowship.

Supplemental Materials

Supplemental materials may be found here:
www.landesbioscience.com/journals/autophagy/article/25188

References

1. Pasinelli P, Brown RH. Molecular biology of amyotrophic lateral sclerosis: insights from genetics. Nat Rev Neurosci 2006; 7:710-23; PMID:16924260; http://dx.doi.org/10.1038/nrn1971
2. Boillée S, Vande Velde C, Cleveland DW. ALS: a disease of motor neurons and their nonneuronal neighbors. Neuron 2006; 52:39-59; PMID:17015226; http://dx.doi.org/10.1016/j.neuron.2006.09.018
3. Andersen PM, Al-Chalabi A. Clinical genetics of amyotrophic lateral sclerosis: what do we really know? Nat Rev Neurol 2011; 7:603-15; PMID:21989245; http://dx.doi.org/10.1038/nrneurol.2011.150
4. Nassif M, Matus S, Castillo K, Hetz C. Amyotrophic lateral sclerosis pathogenesis: a journey through the secretory pathway. Antioxid Redox Signal 2010; 13:1955-89; PMID:20560784; http://dx.doi.org/10.1089/ars.2009.2991
5. Bosco DA, Morfini G, Karabacak NM, Song Y, Gros-Louis F, Pasinelli P, et al. Wild-type and mutant SOD1 share an aberrant conformation and a common pathogenic pathway in ALS. Nat Neurosci 2010; 13:1396-403; PMID:20953194; http://dx.doi.org/10.1038/nn.2660
6. Neumann M, Sampathu DM, Kwong LK, Truax AC, Micsenyi MC, Chou TT, et al. Ubiquitinated TDP-43 in frontotemporal lobar degeneration and amyotrophic lateral sclerosis. Science 2006; 314:130-3; PMID:17023659; http://dx.doi.org/10.1126/science.1134108

7. Deng HX, Zhai H, Bigio EH, Yan J, Fecto F, Ajroud K, et al. FUS-immunoreactive inclusions are a common feature in sporadic and non-SOD1 familial amyotrophic lateral sclerosis. Ann Neurol 2010; 67:739-48; PMID:20517935
8. Menzies FM, Moreau K, Rubinsztein DC. Protein misfolding disorders and macroautophagy. Curr Opin Cell Biol 2011; 23:190-7; PMID:21087849; http://dx.doi.org/10.1016/j.ceb.2010.10.010
9. Mizushima N, Levine B, Cuervo AM, Klionsky DJ. Autophagy fights disease through cellular self-digestion. Nature 2008; 451:1069-75; PMID:18305538; http://dx.doi.org/10.1038/nature06639
10. Sato T, Takeuchi S, Saito A, Ding W, Bamba H, Matsuura H, et al. Axonal ligation induces transient redistribution of TDP-43 in brainstem motor neurons. Neuroscience 2009; 164:1565-78; PMID:19782731; http://dx.doi.org/10.1016/j.neuroscience.2009.09.050
11. Hetz C, Thielen P, Matus S, Nassif M, Court F, Kiffin R, et al. XBP-1 deficiency in the nervous system protects against amyotrophic lateral sclerosis by increasing autophagy. Genes Dev 2009; 23:2294-306; PMID:19762508; http://dx.doi.org/10.1101/gad.1830709
12. Tian F, Morimoto N, Liu W, Ohta Y, Deguchi K, Miyazaki K, et al. In vivo optical imaging of motor neuron autophagy in a mouse model of amyotrophic lateral sclerosis. Autophagy 2011; 7:985-92; PMID:21628996; http://dx.doi.org/10.4161/auto.7.9.16012
13. Li L, Zhang X, Le W. Altered macroautophagy in the spinal cord of SOD1 mutant mice. Autophagy 2008; 4:290-3; PMID:18196963
14. Morimoto N, Nagai M, Ohta Y, Miyazaki K, Kurata T, Morimoto M, et al. Increased autophagy in transgenic mice with a G93A mutant SOD1 gene. Brain Res 2007; 1167:112-7; PMID:17689501; http://dx.doi.org/10.1016/j.brainres.2007.06.045
15. Crippa V, Sau D, Rusmini P, Boncoraglio A, Onesto E, Bolzoni E, et al. The small heat shock protein B8 (HspB8) promotes autophagic removal of misfolded proteins involved in amyotrophic lateral sclerosis (ALS). Hum Mol Genet 2010; 19:3440-56; PMID:20570967; http://dx.doi.org/10.1093/hmg/ddq257
16. Gal J, Ström AL, Kwinter DM, Kilty R, Zhang J, Shi P, et al. Sequestosome 1/p62 links familial ALS mutant SOD1 to LC3 via an ubiquitin-independent mechanism. J Neurochem 2009; 111:1062-73; PMID:19765191; http://dx.doi.org/10.1111/j.1471-4159.2009.06388.x
17. Kabuta T, Suzuki Y, Wada K. Degradation of amyotrophic lateral sclerosis-linked mutant Cu,Zn-superoxide dismutase proteins by macroautophagy and the proteasome. J Biol Chem 2006; 281:30524-33; PMID:16920710; http://dx.doi.org/10.1074/jbc.M603337200
18. Wang X, Fan H, Ying Z, Li B, Wang H, Wang G. Degradation of TDP-43 and its pathogenic form by autophagy and the ubiquitin-proteasome system. Neurosci Lett 2010; 469:112-6; PMID:19944744; http://dx.doi.org/10.1016/j.neulet.2009.11.055
19. Caccamo A, Majumder S, Deng JJ, Bai Y, Thornton FB, Oddo S. Rapamycin rescues TDP-43 mislocalization and the associated low molecular mass neurofilament instability. J Biol Chem 2009; 284:27416-24; PMID:19651785; http://dx.doi.org/10.1074/jbc.M109.031278
20. Fornai F, Longone P, Cafaro L, Kastsiuchenka O, Ferrucci M, Manca ML, et al. Lithium delays progression of amyotrophic lateral sclerosis. Proc Natl Acad Sci U S A 2008; 105:2052-7; PMID:18250315; http://dx.doi.org/10.1073/pnas.0708022105
21. Meissner F, Molawi K, Zychlinsky A. Mutant superoxide dismutase 1-induced IL-1beta accelerates ALS pathogenesis. Proc Natl Acad Sci U S A 2010; 107:13046-50; PMID:20616033; http://dx.doi.org/10.1073/pnas.1002396107
22. Hadano S, Otomo A, Kunita R, Suzuki-Utsunomiya K, Akatsuka A, Koike M, et al. Loss of ALS2/Alsin exacerbates motor dysfunction in a SOD1-expressing mouse ALS model by disturbing endolysosomal trafficking. PLoS One 2010; 5:e9805; PMID:20339559; http://dx.doi.org/10.1371/journal.pone.0009805
23. Chen S, Zhang X, Song L, Le W. Autophagy dysregulation in amyotrophic lateral sclerosis. Brain Pathol 2012; 22:110-6; PMID:22150926; http://dx.doi.org/10.1111/j.1750-3639.2011.00546.x
24. Fecto F, Yan J, Vemula SP, Liu E, Yang Y, Chen W, et al. SQSTM1 mutations in familial and sporadic amyotrophic lateral sclerosis. Arch Neurol 2011; 68:1440-6; PMID:22084127; http://dx.doi.org/10.1001/archneurol.2011.250
25. Deng HX, Chen W, Hong ST, Boycott KM, Gorrie GH, Siddique N, et al. Mutations in UBQLN2 cause dominant X-linked juvenile and adult-onset ALS and ALS/dementia. Nature 2011; 477: 211-5
26. Ferguson CJ, Lenk GM, Meisler MH. Defective autophagy in neurons and astrocytes from mice deficient in PI(3,5)P2. Hum Mol Genet 2009; 18:4868-78; PMID:19793721; http://dx.doi.org/10.1093/hmg/ddp460
27. Komatsu M, Waguri S, Chiba T, Murata S, Iwata J, Tanida I, et al. Loss of autophagy in the central nervous system causes neurodegeneration in mice. Nature 2006; 441:880-4; PMID:16625205; http://dx.doi.org/10.1038/nature04723
28. Hara T, Nakamura K, Matsui M, Yamamoto A, Nakahara Y, Suzuki-Migishima R, et al. Suppression of basal autophagy in neural cells causes neurodegenerative disease in mice. Nature 2006; 441:885-9; PMID:16625204; http://dx.doi.org/10.1038/nature04724
29. Ravikumar B, Vacher C, Berger Z, Davies JE, Luo S, Oroz LG, et al. Inhibition of mTOR induces autophagy and reduces toxicity of polyglutamine expansions in fly and mouse models of Huntington disease. Nat Genet 2004; 36:585-95; PMID:15146184; http://dx.doi.org/10.1038/ng1362
30. Majumder S, Richardson A, Strong R, Oddo S. Inducing autophagy by rapamycin before, but not after, the formation of plaques and tangles ameliorates cognitive deficits. PLoS One 2011; 6:e25416; PMID:21980451; http://dx.doi.org/10.1371/journal.pone.0025416
31. Zhang X, Li L, Chen S, Yang D, Wang Y, Zhang X, et al. Rapamycin treatment augments motor neuron degeneration in SOD1(G93A) mouse model of amyotrophic lateral sclerosis. Autophagy 2011; 7:412-25; PMID:21193837; http://dx.doi.org/10.4161/auto.7.4.14541
32. Laplante M, Sabatini DM. mTOR signaling in growth control and disease. Cell 2012; 149:274-93; PMID:22500797; http://dx.doi.org/10.1016/j.cell.2012.03.017
33. Nassif M, Hetz C. Targeting autophagy in ALS: a complex mission. Autophagy 2011; 7:450-3; PMID:21252621; http://dx.doi.org/10.4161/auto.7.4.14700
34. Bhattacharya A, Bokov A, Muller FL, Jernigan AL, Maslin K, Diaz V, et al. Dietary restriction but not rapamycin extends disease onset and survival of the H46R/H48Q mouse model of ALS. Neurobiol Aging 2012; 33:1829-32; PMID:21763036; http://dx.doi.org/10.1016/j.neurobiolaging.2011.06.002
35. Fleming A, Noda T, Yoshimori T, Rubinsztein DC. Chemical modulators of autophagy as biological probes and potential therapeutics. Nat Chem Biol 2011; 7:9-17; PMID:21164513; http://dx.doi.org/10.1038/nchembio.500
36. Sarkar S, Davies JE, Huang Z, Tunnacliffe A, Rubinsztein DC. Trehalose, a novel mTOR-independent autophagy enhancer, accelerates the clearance of mutant huntingtin and alpha-synuclein. J Biol Chem 2007; 282:5641-52; PMID:17182613; http://dx.doi.org/10.1074/jbc.M609532200
37. Krüger U, Wang Y, Kumar S, Mandelkow EM. Autophagic degradation of tau in primary neurons and its enhancement by trehalose. Neurobiol Aging 2012; 33:2291-305; PMID:22169203; http://dx.doi.org/10.1016/j.neurobiolaging.2011.11.009
38. Gomes C, Escrevente C, Costa J. Mutant superoxide dismutase 1 overexpression in NSC-34 cells: effect of trehalose on aggregation, TDP-43 localization and levels of co-expressed glycoproteins. Neurosci Lett 2010; 475:145-9; PMID:20363292; http://dx.doi.org/10.1016/j.neulet.2010.03.065
39. Lan DM, Liu FT, Zhao J, Chen Y, Wu JJ, Ding ZT, et al. Effect of trehalose on PC12 cells overexpressing wild-type or A53T mutant α-synuclein. Neurochem Res 2012; 37:2025-32; PMID:22707286; http://dx.doi.org/10.1007/s11064-012-0823-0
40. Aguib Y, Heiseke A, Gilch S, Riemer C, Baier M, Schätzl HM, et al. Autophagy induction by trehalose counteracts cellular prion infection. Autophagy 2009; 5:361-9; PMID:19182537; http://dx.doi.org/10.4161/auto.5.3.7662
41. Tanaka M, Machida Y, Niu S, Ikeda T, Jana NR, Doi H, et al. Trehalose alleviates polyglutamine-mediated pathology in a mouse model of Huntington disease. Nat Med 2004; 10:148-54; PMID:14730359; http://dx.doi.org/10.1038/nm985
42. Davies JE, Sarkar S, Rubinsztein DC. Trehalose reduces aggregate formation and delays pathology in a transgenic mouse model of oculopharyngeal muscular dystrophy. Hum Mol Genet 2006; 15:23-31; PMID:16311254; http://dx.doi.org/10.1093/hmg/ddi422
43. Rodríguez-Navarro JA, Rodríguez L, Casarejos MJ, Solano RM, Gómez A, Perucho J, et al. Trehalose ameliorates dopaminergic and tau pathology in parkin deleted/tau overexpressing mice through autophagy activation. Neurobiol Dis 2010; 39:423-38; PMID:20546895; http://dx.doi.org/10.1016/j.nbd.2010.05.014
44. Schaeffer V, Lavenir I, Ozcelik S, Tolnay M, Winkler DT, Goedert M. Stimulation of autophagy reduces neurodegeneration in a mouse model of human tauopathy. Brain 2012; 135:2169-77; PMID:22689910; http://dx.doi.org/10.1093/brain/aws143
45. Perucho J, Casarejos MJ, Gomez A, Solano RM, de Yébenes JG, Mena MA. Trehalose protects from aggravation of amyloid pathology induced by isoflurane anesthesia in APP(swe) mutant mice. Curr Alzheimer Res 2012; 9:334-43; PMID:22272607; http://dx.doi.org/10.2174/156720512800107573
46. Vidal RL, Figueroa A, Court FA, Thielen P, Molina C, Wirth C, et al. Targeting the UPR transcription factor XBP1 protects against Huntington's disease through the regulation of FoxO1 and autophagy. Hum Mol Genet 2012; 21:2245-62; PMID:22337954; http://dx.doi.org/10.1093/hmg/dds040
47. Sadagurski M, Cheng Z, Rozzo A, Palazzolo I, Kelley GR, Dong X, et al. IRS2 increases mitochondrial dysfunction and oxidative stress in a mouse model of Huntington disease. J Clin Invest 2011; 121:4070-81; PMID:21926467; http://dx.doi.org/10.1172/JCI46305
48. Xu P, Das M, Reilly J, Davis RJ. JNK regulates FoxO-dependent autophagy in neurons. Genes Dev 2011; 25:310-22; PMID:21325132; http://dx.doi.org/10.1101/gad.1984311
49. Sengupta A, Molkentin JD, Yutzey KE. FoxO transcription factors promote autophagy in cardiomyocytes. J Biol Chem 2009; 284:28319-31; PMID:19696026; http://dx.doi.org/10.1074/jbc.M109.024406

50. Rzymski T, Milani M, Pike L, Buffa F, Mellor HR, Winchester L, et al. Regulation of autophagy by ATF4 in response to severe hypoxia. Oncogene 2010; 29:4424-35; PMID:20514020; http://dx.doi.org/10.1038/onc.2010.191
51. Rouschop KM, van den Beucken T, Dubois L, Niessen H, Bussink J, Savelkouls K, et al. The unfolded protein response protects human tumor cells during hypoxia through regulation of the autophagy genes MAP1LC3B and ATG5. J Clin Invest 2010; 120:127-41; PMID:20038797; http://dx.doi.org/10.1172/JCI40027
52. Milani M, Rzymski T, Mellor HR, Pike L, Bottini A, Generali D, et al. The role of ATF4 stabilization and autophagy in resistance of breast cancer cells treated with Bortezomib. Cancer Res 2009; 69:4415-23; PMID:19417138; http://dx.doi.org/10.1158/0008-5472.CAN-08-2839
53. Matus S, Lopez E, Valenzuela V, Nassif M, Hetz C. Functional contribution of the transcription factor ATF4 to the pathogenesis of amyotrophic lateral sclerosis. Plos One 2013; In press
54. Zhou Y, Lee J, Reno CM, Sun C, Park SW, Chung J, et al. Regulation of glucose homeostasis through a XBP-1-FoxO1 interaction. Nat Med 2011; 17:356-65; PMID:21317886; http://dx.doi.org/10.1038/nm.2293
55. Klionsky DJ, Abdalla FC, Abeliovich H, Abraham RT, Acevedo-Arozena A, Adeli K, et al. Guidelines for the use and interpretation of assays for monitoring autophagy. Autophagy 2012; 8:445-544; PMID:22966490; http://dx.doi.org/10.4161/auto.19496
56. Ilieva H, Polymenidou M, Cleveland DW. Non-cell autonomous toxicity in neurodegenerative disorders: ALS and beyond. J Cell Biol 2009; 187:761-72; PMID:19951898; http://dx.doi.org/10.1083/jcb.200908164
57. Seglen PO, Gordon PB. 3-Methyladenine: specific inhibitor of autophagic/lysosomal protein degradation in isolated rat hepatocytes. Proc Natl Acad Sci U S A 1982; 79:1889-92; PMID:6952238; http://dx.doi.org/10.1073/pnas.79.6.1889
58. Nagai M, Re DB, Nagata T, Chalazonitis A, Jessell TM, Wichterle H, et al. Astrocytes expressing ALS-linked mutated SOD1 release factors selectively toxic to motor neurons. Nat Neurosci 2007; 10:615-22; PMID:17435755; http://dx.doi.org/10.1038/nn1876
59. Di Giorgio FP, Carrasco MA, Siao MC, Maniatis T, Eggan K. Non-cell autonomous effect of glia on motor neurons in an embryonic stem cell-based ALS model. Nat Neurosci 2007; 10:608-14; PMID:17435754; http://dx.doi.org/10.1038/nn1885
60. Haidet-Phillips AM, Hester ME, Miranda CJ, Meyer K, Braun L, Frakes A, et al. Astrocytes from familial and sporadic ALS patients are toxic to motor neurons. Nat Biotechnol 2011; 29:824-8; PMID:21832997; http://dx.doi.org/10.1038/nbt.1957
61. Fritz E, Izaurieta P, Weiss A, Mir FR, Rojas P, Gonzalez D, et al. Mutant SOD1-expressing astrocytes release toxic factors that trigger motoneuron death by inducing hyperexcitability. J Neurophysiol 2013; 109:2803-14; PMID:23486205; http://dx.doi.org/10.1152/jn.00500.2012
62. Kroemer G, Mariño G, Levine B. Autophagy and the integrated stress response. Mol Cell 2010; 40:280-93; PMID:20965422; http://dx.doi.org/10.1016/j.molcel.2010.09.023
63. Bellingham MC. A review of the neural mechanisms of action and clinical efficiency of riluzole in treating amyotrophic lateral sclerosis: what have we learned in the last decade? CNS Neurosci Ther 2011; 17:4-31; PMID:20236142; http://dx.doi.org/10.1111/j.1755-5949.2009.00116.x
64. Harris H, Rubinsztein DC. Control of autophagy as a therapy for neurodegenerative disease. Nat Rev Neurol 2012; 8:108-17; PMID:22187000; http://dx.doi.org/10.1038/nrneurol.2011.200
65. Wang IF, Guo BS, Liu YC, Wu CC, Yang CH, Tsai KJ, et al. Autophagy activators rescue and alleviate pathogenesis of a mouse model with proteinopathies of the TAR DNA-binding protein 43. Proc Natl Acad Sci U S A 2012; 109:15024-9; PMID:22932872; http://dx.doi.org/10.1073/pnas.1206362109
66. Gill A, Kidd J, Vieira F, Thompson K, Perrin S. No benefit from chronic lithium dosing in a sibling-matched, gender balanced, investigator-blinded trial using a standard mouse model of familial ALS. PLoS One 2009; 4:e6489; PMID:19649300; http://dx.doi.org/10.1371/journal.pone.0006489
67. Pizzasegola C, Caron I, Daleno C, Ronchi A, Minoia C, Carrì MT, et al. Treatment with lithium carbonate does not improve disease progression in two different strains of SOD1 mutant mice. Amyotroph Lateral Scler 2009; 10:221-8; PMID:19308767; http://dx.doi.org/10.1080/17482960902803440
68. Verstraete E, Veldink JH, Huisman MH, Draak T, Uijtendaal EV, van der Kooi AJ, et al. Lithium lacks effect on survival in amyotrophic lateral sclerosis: a phase IIb randomised sequential trial. J Neurol Neurosurg Psychiatry 2012; 83:557-64; PMID:22378918; http://dx.doi.org/10.1136/jnnp-2011-302021
69. Chiò A, Borghero G, Calvo A, Capasso M, Caponnetto C, Corbo M, et al.; LITALS Study Group. Lithium carbonate in amyotrophic lateral sclerosis: lack of efficacy in a dose-finding trial. Neurology 2010; 75:619-25; PMID:20702794; http://dx.doi.org/10.1212/WNL.0b013e3181ed9e7c
70. Matus S, Glimcher LH, Hetz C. Protein folding stress in neurodegenerative diseases: a glimpse into the ER. Curr Opin Cell Biol 2011; 23:239-52; PMID:21288706; http://dx.doi.org/10.1016/j.ceb.2011.01.003
71. Brotherton TE, Li Y, Glass JD. Cellular toxicity of mutant SOD1 protein is linked to an easily soluble, non-aggregated form in vitro. Neurobiol Dis 2012; 49C:49-56; PMID:22926189
72. Hetz C, Thielen P, Fisher J, Pasinelli P, Brown RH, Korsmeyer S, et al. The proapoptotic BCL-2 family member BIM mediates motoneuron loss in a model of amyotrophic lateral sclerosis. Cell Death Differ 2007; 14:1386-9; PMID:17510659; http://dx.doi.org/10.1038/sj.cdd.4402166
73. Ludolph AC, Bendotti C, Blaugrund E, Chio A, Greensmith L, Loeffler JP, et al. Guidelines for preclinical animal research in ALS/MND: A consensus meeting. Amyotroph Lateral Scler 2010; 11:38-45; PMID:20184514; http://dx.doi.org/10.3109/17482960903545334
74. Hetz C, Lee AH, Gonzalez-Romero D, Thielen P, Castilla J, Soto C, et al. Unfolded protein response transcription factor XBP-1 does not influence prion replication or pathogenesis. Proc Natl Acad Sci U S A 2008; 105:757-62; PMID:18178615; http://dx.doi.org/10.1073/pnas.0711094105
75. Valenzuela V, Collyer E, Armentano D, Parsons GB, Court FA, Hetz C. Activation of the unfolded protein response enhances motor recovery after spinal cord injury. Cell Death Dis 2012; 3:e272; PMID:22337234; http://dx.doi.org/10.1038/cddis.2012.8
76. Barrientos SA, Martinez NW, Yoo S, Jara JS, Zamorano S, Hetz C, et al. Axonal degeneration is mediated by the mitochondrial permeability transition pore. J Neurosci 2011; 31:966-78; PMID:21248121; http://dx.doi.org/10.1523/JNEUROSCI.4065-10.2011
77. Cashman NR, Durham HD, Blusztajn JK, Oda K, Tabira T, Shaw IT, et al. Neuroblastoma x spinal cord (NSC) hybrid cell lines resemble developing motor neurons. Dev Dyn 1992; 194:209-21; PMID:1467557; http://dx.doi.org/10.1002/aja.1001940306
78. Pankiv S, Clausen TH, Lamark T, Brech A, Bruun JA, Outzen H, et al. p62/SQSTM1 binds directly to Atg8/LC3 to facilitate degradation of ubiquitinated protein aggregates by autophagy. J Biol Chem 2007; 282:24131-45; PMID:17580304; http://dx.doi.org/10.1074/jbc.M702824200
79. Sepulveda FJ, Bustos FJ, Inostroza E, Zúñiga FA, Neve RL, Montecino M, et al. Differential roles of NMDA Receptor Subtypes NR2A and NR2B in dendritic branch development and requirement of RasGRF1. J Neurophysiol 2010; 103:1758-70; PMID:20107120; http://dx.doi.org/10.1152/jn.00823.2009